Simulation of Radar Micro-Doppler Patterns for Multi-Propeller Drones

Yefeng Cai[+1,+2], Oleg Krasnov[*3], Alexander Yarovoy[#4]
Faculty of Electrical Engineering, Mathematics and Computer Science
Delft University of Technology
Delft, The Netherlands
[+1]*y.cai-2@student.tudelft.nl*, [+2]*yefeng.cai@hotmail.com*, {[*3]*o.a.krasnov*, [#4]*a.yarovoy*}*@tudelft.nl*

***Abstract*—This paper presents a thin-wire electromagnetic (EM) model of multi-propeller drone that generates drone micro-Doppler pattern efficiently as a function of radar parameters and propeller properties. Experimental results of propeller micro-Doppler pattern measured in anechoic chamber was investigated and used to validate the results produced by thin-wire model of single propeller in S-band and X-band. Then the thin-wire model was expanded to multi-propeller drones and reproduced linear micro-Doppler patterns of multi-propeller drone measured by radar system in long Coherent Processing Interval (CPI) circumstance. The model-based replica was shown to be useful in radar micro-Doppler analysis of multi-propeller drones, especially to study the influence of propellers synchronisation and in long CPI circumstances.**

***Index Terms*—electromagnetic, drone, micro-Doppler, radar, CPI**

I. Introduction

In the last few years, the usage of drones has increased dramatically. Low price and easy operation have spread drones to many domains, such as aerial photography, land mapping, disaster rescue, etc, raising concerns of risks in flight safety, air security and privacy issues.

In order to detect and classify drones, radar micro-Doppler analysis is widely used. In this case, the radar systems observe the micro-Doppler spectral components introduced by rotating parts of the drone. Analysis of these components reveals the properties of rotating parts, such as the number and angular speed of rotors, the length of propeller blades and their synchronization.

Various methods have been used to collect micro-Doppler data. In [1], the authors measured the reflected signals of helicopter, quadcopter and hexacopter drones and showed their micro-Doppler patterns. In that work, the drones were fixed indoor near radar antennas, guaranteeing clear periodic micro-Doppler patterns of high signal to noise ratio (SNR), yet clear periodic patterns are not always available in the noisy environment. Speirs et al. presented in [2] periodic micro-Doppler patterns of quadcopter using fine and simplified simulation models. However, the propellers considered in that work were rotating in the same velocity with constant angle shift, while they may have different angles and velocities in practice. Ritchie et al. in [3] simulated propeller RCS which may lead to micro-Doppler pattern with further processing. However, the simulation requires much time even for a single propeller.

In reality, synchronization of drone propellers in angles and velocities have an influence on drone micro-Doppler pattern. Besides, using long CPI in Doppler processing improves the SNR of a micro-Doppler image but ruins periodic details of the pattern and leads to linear instead of the quasi-sinusoidal micro-Doppler pattern [4]. Generally, real measured data of drone micro-Doppler pattern highly depends on specific drones and radar setups, while software simulation containing flexible parameters is quite time-consuming. In order to investigate these issues, this paper develops a computationally efficient analytical model that is valid under various setups in demand to generate micro-Doppler patterns.

The paper is organized as follows. Section II presents the experimental results of propeller micro-Doppler pattern and proposes a thin-wire EM model to reproduce the micro-Doppler pattern. Section III presents the micro-Doppler pattern of a drone measured by the radar system and expands the thin-wire model to multi-propeller drones. In Section IV, model-based micro-Doppler patterns are discussed, especially in propeller synchronization and long CPI circumstances. Section V describes the conclusions and future works.

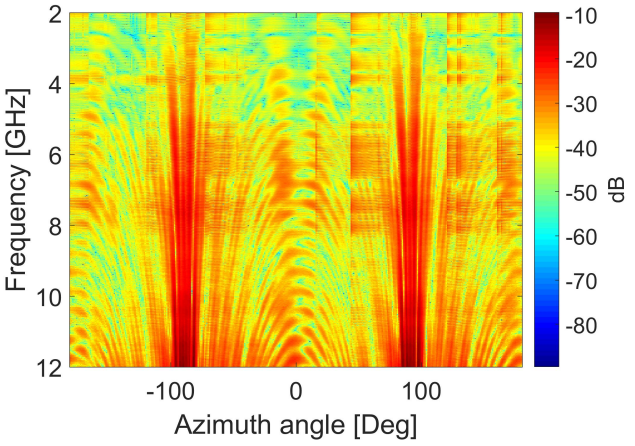

Fig. 1: Measured the angular-frequency dependence of the DJI R2170 propeller's RCS

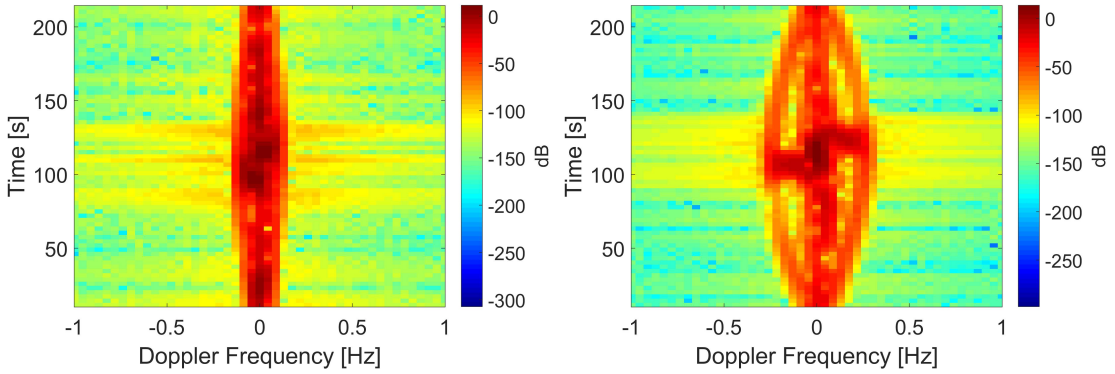

Fig. 2: The micro-Doppler patterns of the DJI R2170 propeller that are simulated based on measured in the TU Delft DUCAT anechoic chamber complex backscattered signals at: (a) 3.315 GHz, (b) 10 GHz

II. Radar signal scattering on single propeller: Experiment and Simulations

In order to study the micro-Doppler pattern of radar signal that is scattered on a drone with specific design geometry and motion parameters as a function of radar configuration and signal processing chain's setup, it is necessary to investigate the angular dependence of backscattered radar signal from a typical propeller. Such a dependence then can be easily converted into micro-Doppler pattern of rotated with specific angular velocity Ω propeller that is observed by a radar with specific parameters of sensing signals like pulse repetition interval (PRI) and Doppler coherent processing interval (CPI).

The complex backscattered signals of the DJI R2170 propeller was measured in the TU Delft DUCAT EM anechoic chamber (see Fig.1). This propeller is a representative of most popular two-blade propellers [5]. For the measurements the propeller was placed at 3.3 m distance from the Tx/Rx antennas and rotated in 450 seconds from -180° to 180° with a step of 0.036°. For every angular position a vector network analyser (VNA) recorded 21 samples of reflection coefficient sweeping from 2 GHz (S-band) to 12 GHz (X-band). This frequency interval from S-band to X-band was selected because it is most used in radar systems of air traffic control, weather monitoring and target tracking. During the measurement campaign the chamber's background and the RCS of 0.2 m by 0.2 m metal plate were also measured for calibration. The calibrated propeller's RCS has been evaluated using equation as follows

$$\sigma_{prop} = \sigma_{mp} \cdot \frac{P_{r,prop}}{P_{t,prop}} \cdot \frac{P_{t,mp}}{P_{r,mp}}, \tag{1}$$

where σ_{mp} is the known RCS of metal plate, $P_{r,mp}$ and $P_{t,mp}$ are the received and transmitted power of metal plate, and $P_{r,prop}$ and $P_{t,prop}$ are the received and transmitted power of propeller. As can be seen from the Fig.1, the maximum RCS appears at $\pm 90°$ when the propeller is perpendicular to the radar's line of sight (LOS).

Applying to the measured on specific frequency complex reflection coefficient data the 1,024-point Short-Time Fourier transform (STFT) with 896 overlapped points simulates the micro-Doppler patterns of slowly rotated with angular velocity $\Omega = 0.13$ rpm propeller that is observed by a radar with at 3.315 GHz and 10 GHz carrier frequency, PRF $= 22$ Hz and CPI $= 46.08$ s (see Fig.2).

Another beneficial approach to study micro-Doppler radar characteristics of drones can be based on electromagnetic simulations of angular dependence of the propellers reflection coefficients at specific frequency and polarization. Such simulations can be based on running of computationally complex electromagnetic solvers (like FEKO) with precise 3D CAD model of propeller, or on simplified models that reproduce only most important behaviour of scattering characteristics. As an example of second approach, a thin-wire model ($\varnothing \ll \lambda$ [6]) has been proposed to simulate micro-Doppler patterns of the reflected on rotating wind turbine blades radar signals [4]. In the same style, the model-based reflected signal of drone's rotating propeller is a function of time t and variables of propeller properties, given as

$$\begin{aligned} E^{prop}(t, r_p, \theta_{b,w}, l_{b,w}) &\sim \sum_{b=1}^{B} E_b^{blade}(t, r_p, \theta_{b,w}, l_{b,w}) \\ &= \sum_{b=1}^{B} \sum_{w=1}^{W} E_{b,w}^{wire}(t, r_p, \theta_{b,w}, l_{b,w}) \\ &= \sum_{b=1}^{B} \sum_{w=1}^{W} \int_0^{l_{b,w}} j\eta \frac{k e^{-jkr_p}}{4\pi r_p} \\ &\times E_{r_p}^{in}(t) \sin(\theta_{b,w} + \Omega t) \\ &\times e^{j2kz'_{b,w} cos(\theta_{b,w} + \Omega t)} dz'_{b,w} \end{aligned} \tag{2}$$

where symbol $\sim$ indicates proportionality, $\eta = 120\pi$ is the intrinsic impedance of air, $k = 2\pi/\lambda$ is wavenumber. r_p is the distance from propeller rotation centre to an observation point.

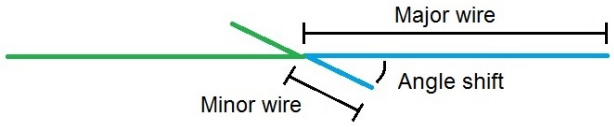

Fig. 3: Thin-wire model of the DJI R2170 propeller

B is the number of blades per propeller, W is the number of thin wires per blade in the simplified model, $dz'_{b,w}$ is the length of infinitesimal dipole along the z-axis at the distance $z'_{b,w}$ along the w^{th} wire of the b^{th} blade in the rotation plane. $l_{b,w}$ is the length of the w^{th} wire of the b^{th} blade. The propeller rotates with the angular velocity Ω and all angles changes in time linearly: $\theta(t) = \theta_{b,w} + \Omega t$, where $\theta_{b,w}$ is the initial angle of the w^{th} wire of the b^{th} blade relatively to the LOS at time $t = 0$. W, $\theta_{b,w}$ and $l_{b,w}$ depend on the design geometry of propeller.

This model focuses on the phase of reflected signal and omits the magnitude factor, because phase factor contains propeller rotation information influencing final micro-Doppler patterns. Only horizontal-horizontal (HH) polarisation is considered in the model, since both the geometry and rotation of propeller is most in horizontal plane.

To apply this simplified model to the DJI R2170 propeller, each blade was represented as two thin wires, according to the blade's geometry, of 0.267 m and 0.053 m in length and 15° shifted in angle (see Fig.3). A signal series of 100,000 complex values at specific frequency was generated assuming the propeller rotating from 0° to 180° in 225 seconds. The model-based micro-Doppler pattern was simulated by applying 10,240-point STFT to the generated series with 8,960 points overlapped.

As can be seen from comparison of Fig. 2 and 4, the simulated model-based micro-Doppler patterns are almost the same as their measured counterparts. In Fig.4, the micro-Doppler patterns are invisible from the background when the propeller blade is approximately perpendicular to LOS, because in the analytical model the computed backscattered signals are about zero at these moments. In Fig.2, the micro-Doppler patterns are clearly presented due to the good dynamic range of experimental equipment. The chamber background is below -50 dB, while propeller scattered signals are between -40 dB and -10 dB .

Overall, the thin-wire model reproduces valid micro-Doppler patterns at X-band and S-band, given specific variables of propeller properties and radar setups.

III. Radar signal scattering on multi-propeller drone: Experiment and Simulations

The drone-reflected EM signal contributing to micro-Doppler pattern is the synthesis of signals reflected by multiple propellers. The Fig. 5 presents the geometrical design of a quadcopter as an example, with all four propellers represented with a simplified model (see Fig.3) as in Eq. (2). The synthetic reflected signal of the quadcopter, as a combination of several propeller reflections, is given as

$$\begin{aligned} E^{drone}(t, r_0) &\sim \sum_{p=1}^{P} E_p^{prop}(t, r_p, \theta_{p,b,w}, l_{p,b,w}) \\ &= \sum_{p=1}^{P}\sum_{b=1}^{B}\sum_{w=1}^{W} E_{p,b,w}^{wire}(t, r_p, \theta_{p,b,w}, l_{p,b,w}) \\ &= \sum_{p=1}^{P}\sum_{b=1}^{B}\sum_{w=1}^{W} \int_0^{l_{p,b,w}} j\eta \frac{k e^{-jkr_p}}{4\pi r_p} \\ &\times E_{r_0}^{in}(t)\sin(\theta_{p,b,w} + \Omega_p t) \\ &\times e^{j2kz'_{p,b,w}cos(\theta_{p,b,w}+\Omega_p t)} dz'_{p,b,w} \end{aligned} \tag{3}$$

where most symbols and variables are defined the same as in Eq. (2). In this equation $dz'_{p,b,w}$, $l_{p,b,w}$ and $\theta_{p,b,w}$ are specified for each of P propellers.

Indexed parameters Ω_p and r_p make Eq. (3) different from Eq. (2). Parameter Ω_p is the rotation velocity of p^{th} propeller. When the drone makes any maneuver, propellers become asynchronous in velocity, and Ω_ps are different from each others. r_p is the radial distance from p^{th} propeller rotation centre to observation point. If we define within drone's geometry design some center point O with the distance r_0 to the remote observation point and some reference axis (see Fig.5), we can relate the radial distances r_p to the drone distance r_0, the drone observation angle α_0 and the geometrical structure of multi-propeller drone

$$r_p = r_0 - d_p \cdot cos(\alpha_p - \alpha_0). \tag{4}$$

Here d_p is the length from the rotation centre of the p^{th} propeller to drone centre, α_0 is the angle between drone's reference axis and LOS, and α_p is the angle between the p^{th} propeller arm OB and reference axis. Reference axis is set at the first propeller arm OA in this example. The distance between drone centre and propeller centre is considered in this model, because it introduces additional phase shift to scattered EM signal. Besides, to make the figure clear, in Fig.5, only the start angle and length of the major wire of the p^{th} propeller's first blade are shown as θ_p and l_p. Details of each simplified propeller are the same as in Eq.(2).

To validate the thin-wire model of multi-propeller drone and its micro-Doppler pattern, the real backscattered signal of DJI M600 drone [7] was measured using PARSAX radar system mounted on the roof of EWI building on TU Delft campus [8] [9]. The radar was configured to take full polarimetric measurements simultaneously at the single centre frequency f_c = 3.315 GHz with pulse repetition frequency PRF = 1 kHz. The dish antenna with a beamwidth of 1.8° was elevated for 0.9° to avoid ground clutter. The drone was set 9 km away from the radar antennas, hovering steadily within the beamwidth. Micro-Doppler pattern of the drone was achieved by applying 256-point STFT to a received signal series of 2 seconds with 128 points overlapped.

Drone micro-Doppler pattern was also generated from the thin-wire model. A synthetic backscattered signal series of 6

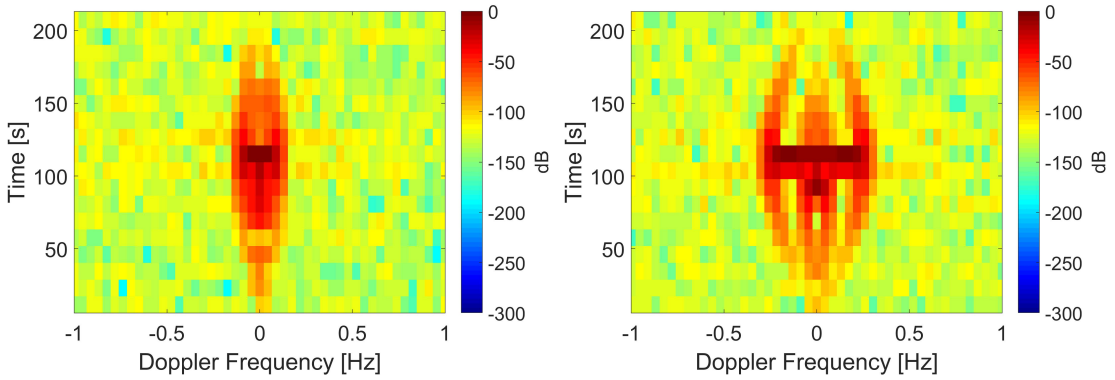

Fig. 4: The micro-Doppler patterns of the DJI R2170 propeller that are simulated based on thin-wire model (2) at: (a) 3.315 GHz, (b) 10 GHz

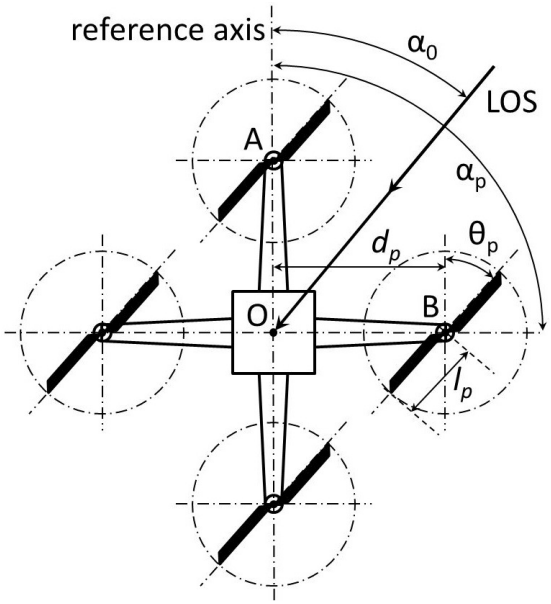

Fig. 5: The geometrical design of a quadcopter as an example of multi-propeller drone

DJI R2170 propellers were generated with sampling frequency f_s = 1 kHz. The propellers were assumed rotating with random angle shift at the same velocity of 3000 rpm which is reasonable for drones. The model-based micro-Doppler pattern was achieved by applying 256-point STFT to the generated signal series of 2 seconds with 128 points overlapped. Fig.6 shows the normalised micro-Doppler patterns in HH polarisation measured by real radar system and generated from the thin-wire model.

In these circumstances, the micro-Doppler patterns are linear instead of periodic quasi-sinusoidal, because the CPI (256 ms) is much longer than propeller rotation period (20 ms) and the periodic rotation detail is lost. The frequency resolution, temporal stability and SNR of model-based micro-Doppler pattern in Fig.6b are better than those in Fig.6a measured by real radar system. Possible reasons for this difference are the dynamic range of radar system and the far distance, noisy environment and air disturbance in open air.

Overall, the thin-wire model reproduces reliable micro-Doppler patterns in long CPI circumstances, in terms of the distribution of linear patterns over the Doppler bandwidth.

IV. Discussion on Results of Micro-Doppler Patterns

Thin-wire model of radar signal scattering on propeller and its micro-Doppler patterns were presented. The model simplified propeller blade as two thin wires, according to the blade number, blade length and blade geometry structure of a real propeller. The contribution of these variables of propeller property was shown in model-based micro-Doppler patterns. More wires can be used and should lead to better simulation results for different propellers, though there is a trade-off between model complexity and efficiency, and the design of wire lengths and wire angle shifts takes additional efforts. The model is valid at S-band and X-band. Within other radar bandwidth, the model needs further validation and may be too simple to describe scattered EM signals in detail. However, for radar frequency from several to dozens of GHz, this model has been shown reliably reflecting propeller variables on micro-Doppler pattern.

Thin-wire model of radar signal scattering on multi-propeller drone and its micro-Doppler pattern in variable CPI circumstance were proposed. The multi-propeller drone model considered the geometry structure of drone as well as propeller synchronisation in angle and velocity. Real drone measurement was made by radar system in long CPI circumstance, when signal integration time is much longer than the period of propellers rotation. In this circumstance, the model was validated reproducing the linear micro-Doppler patterns.

The model-based micro-Doppler pattern is useful for radar systems observing multi-propeller drones, due to its efficiency and flexibility. Long CPI setup mentioned above is consistent

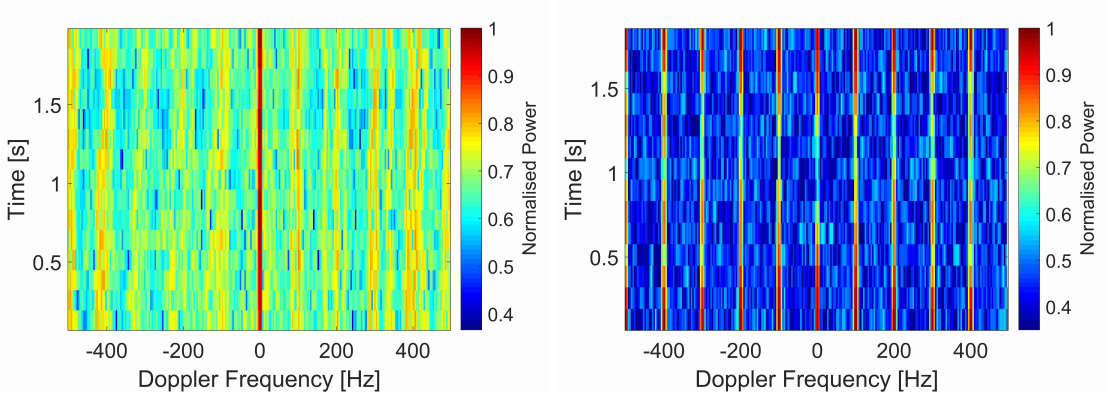

(a) (b)

Fig. 6: The micro-Doppler patterns of the DJI M600 drone: (a) Measured, (b) Model-based

with many practical scenarios. Drone propellers are usually small in diameter of centimetres and rotate fast in velocity of thousands rpm. For radar systems of several kHz PRF, a long integration time is necessary to achieve micro-Doppler patterns with high SNR, especially with drones far away from radar antennas. Given integration time larger than propeller rotation period and probably over several rotation periods, the drone micro-Doppler patterns are linear instead of periodic quasi-sinusoidal. However, these circumstances are not widely investigated, partly because of the lack of observation data. Propellers asynchronous in velocity is another common scenario in practice when a drone is maneuvering, and it has a large influence on micro-Doppler pattern. But the synchronisation of propellers in velocity is not widely discussed, due to the difficulty to observe maneruvering drones with radar systems. The proposed thin-wire multi-propeller model may generate data of micro-Doppler patterns for preliminary discussions on these scenarios.

V. Conclusions

This paper proposed a thin-wire model to efficiently generate micro-Doppler patterns of multi-rotor drones, given specific drone variables and radar parameters. RCS of a drone propeller was measured in anechoic chamber at S-band and X-band. Micro-Doppler pattern of propeller was achieved by performing STFT on the measured RCS signal at sequential angles. A thin-wire model of single propeller was presented to generate backscattered EM signal of the propeller. Micro-Doppler patterns achieved from the model reproduced the experimental results and reflected the propeller variables, such as blade length and blade number. The thin-wire model of single propeller was then expanded to multi-propeller drones, considering more parameters, such as observation angle, drone geometry structure and propeller synchronisation in angle and velocity. Backscattered signal and micro-Doppler pattern of a drone were measured by radar system using long integration time. In this circumstance, the micro-Doppler pattern was linear instead of periodic. The thin-wire model reproduced the measured linear patterns and gave the same pattern frequency distribution. The thin-wire model was shown useful for analysing the influence of drone and propeller properties on radar micro-Doppler patterns, especially in long CPI circumstances.

A natural expansion for this work would be using this thin-wire drone model to investigate linear micro-Doppler patterns. This should include generating micro-Doppler patterns taking various combinations of input variables, such as different drone types and propellers synchronisation. The focus of this would be analysing the influence of these variables on linear micro-Doppler patterns in long CPI circumstances, with the aim of proposing suitable features to characterise linear micro-Doppler patterns for future usage.

Acknowledgements

The authors would like to thank Pascal Aubry and Fred van der Zwan for their supports in anechoic chamber and PARSAX radar measurements and data collection.

References

[1] P. Zhang, L. Yang, G. Chen, and G. Li, "Classification of drones based on micro-Doppler signatures with dual-band radar sensors," in *Progress in Electromagnetics Research Symposium-Fall (PIERS-FALL), 2017*. IEEE, 2017, pp. 638–643.

[2] P. J. Speirs, A. Schröder, M. Renker, P. Wellig, and A. Murk, "Comparisons between simulated and measured X-band signatures of quad-, hexa- and octocopters," in *2018 15th European Radar Conference (EuRAD)*. IEEE, 2018, pp. 325–328.

[3] M. Ritchie, F. Fioranelli, H. Griffiths, and B. Torvik, "Micro-drone RCS analysis," in *Radar Conference, 2015 IEEE*. IEEE, 2015, pp. 452–456.

[4] O. A. Krasnov and A. G. Yarovoy, "Radar micro-Doppler of wind turbines: simulation and analysis using rotating linear wire structures," *International Journal of Microwave and Wireless Technologies*, vol. 7, no. 3-4, pp. 459–467, 2015.

[5] "DJI R2170," https://store.dji.com/product/2170-carbon-fiber-reinforced-folding-propeller-ccw-set, 2019.

[6] C. Balanis, *Antenna Theory: Analysis and Design*. New York: Wiley, 2005.

[7] "DJI Matrice 600 drone. User Manual," on-line https://www.dji.com/nl/matrice600, 2019.

[8] O. A. Krasnov, L. P. Ligthart, Z. Li, P. Lys, and W. F. van der Zwan, "The PARSAX - full polarimetric FMCW radar with dual-orthogonal signals," in *EuRAD. European Microwave Week 2008*, 2008, pp. 84–87.

[9] "PARSAX," on-line http://radar.ewi.tudelft.nl/Facilities/parsax.php, 2019.